Hindawi Publishing Corporation
EURASIP Journal on Wireless Communications and Networking
Volume 2010, Article ID 805216, 16 pages
doi:10.1155/2010/805216

Research Article

Analysis and Construction of Full-Diversity Joint Network-LDPC Codes for Cooperative Communications

Dieter Duyck,[1] Daniele Capirone,[2] Joseph J. Boutros,[3] and Marc Moeneclaey[1]

[1] *Department of Telecommunications and Information Processing, Ghent University, St-Pietersnieuwstraat 41, B-9000 Gent, Belgium*
[2] *Department of Electronics, Politecnico di Torino, Corso Duca Degli Abruzzi 24, 10129 Torino, Italy*
[3] *Electrical Engineering Department, Texas A&M University at Qatar, 23874 Doha, Qatar*

Correspondence should be addressed to Dieter Duyck, dieter.duyck@telin.ugent.be

Received 29 December 2009; Revised 14 April 2010; Accepted 3 June 2010

Academic Editor: Christoph Hausl

Transmit diversity is necessary in harsh environments to reduce the required transmit power for achieving a given error performance at a certain transmission rate. In networks, cooperative communication is a well-known technique to yield transmit diversity and network coding can increase the spectral efficiency. These two techniques can be combined to achieve a double diversity order for a maximum coding rate $R_c = 2/3$ on the Multiple-Access Relay Channel (MARC), where two sources share a common relay in their transmission to the destination. However, codes have to be carefully designed to obtain the intrinsic diversity offered by the MARC. This paper presents the principles to design a family of full-diversity LDPC codes with maximum rate. Simulation of the word error rate performance of the new proposed family of LDPC codes for the MARC confirms the full diversity.

1. Introduction

Multipath propagation (small-scale fading) is an important salient effect of wireless channels, causing possible destructive adding of signals at the receiver. When the fading varies very slowly, error-correcting codes cannot combat the detrimental effect of the fading on a point-to-point channel. Space diversity, that is, transmitting information over independent paths in space, is a means to mitigate the effects of slowly varying fading. Cooperative communication [1–4] is a well-known technique to yield transmit diversity. The most elementary example of a cooperative network is the relay channel, consisting of a source, a relay, and a destination [3, 5]. The task of the relay is specified by the strategy or protocol. In the case of coded cooperation [4], the relay decodes the message received from the source, and then transmits to the destination additional parity bits related to the message; this results in a higher information theoretic spectral efficiency than simply repeating the message received from the source [6]. The resulting outage probability [7] exhibits twice the diversity, as compared to point-to-point transmission. However, the overall error-correcting code should be carefully designed in order to guarantee full diversity [8].

We focus on capacity achieving codes, more precisely, low-density parity-check (LDPC) codes [9], because their word error rate (WER) performance is quasi-independent of the block length [10] when the block length is becoming very large.

Considering two users, S_1 and S_2, and a common destination D, a double diversity order can be obtained by cooperating. When no *common* relay R is used, the maximum achievable coding rate that allows to achieve full diversity is $R_c = 0.5$ (according to the blockwise Singleton bound [7, 11]). However, when one common relay R for two users is used (a Multiple Access Relay Channel—MARC), it can be proven that the maximum achievable coding rate yielding full diversity is $R_c = 2/3$ [12]. The increase of the maximum coding rate yielding full diversity from $R_c = 0.5$ to $R_c = 2/3$ is achieved through network coding [13] at the physical layer, that is, R sends a transformation of its incoming bit packets to D (only linear transformations over GF(5) are considered here). From a decoding point of view, this linear transformation can be interpreted as additional parity bits of a linear block code. Hence, the destination will decode a joint network-channel code. Therefore, the problem formulation is how to design a full-diversity joint network-channel code construction for a rate $R_c = 2/3$.

Up till now, no family of full-diversity LDPC codes with $R_c = 2/3$ for coded cooperation on the MARC has been published. Chebli, Hausl, and Dupraz obtained interesting results on joint network-channel coding for the MARC with turbo codes [14] and LDPC codes [15, 16], but these authors do not elaborate on a structure to guarantee full diversity at maximum rate, which is the most important criterion for a good performance on fading channels. A full-diversity code structure describes a family of LDPC codes or an ensemble of LDPC codes, permitting to generate many specific instances of LDPC codes.

In this paper, we present a strategy to produce excellent LDPC codes for the MARC. First, we outline the physical layer network coding framework. Then, we derive the conditions on the MARC model and the coding rate necessary to achieve a double diversity order. In the second part of the paper, we elaborate on the code construction. A joint network-channel code construction is derived that guarantees full diversity, irrespective of the parameters of the LDPC code (the degree distributions). Finally, the coding gain can be improved by selecting the appropriate degree distributions of the LDPC code [17] or using the *doping* technique [18] as shown in Section 7.2. Simulation results for finite and infinite length (through density evolution) are provided. To the best of authors' knowledge, this is the first time that a joint full-diversity network-channel LDPC code construction for maximum rate is proposed.

Channel-State Information is assumed to be available only at the decoder. In order to simplify the analysis, we consider orthogonal half-duplex devices that transmit in separate timeslots.

2. System Model and Notation

2.1. Multiple Access Relay Channel. We consider a Multiple Access Relay Channel (MARC) with two users S_1 and S_2, a common relay R, and a common destination D. Each of the three transmitting devices transmits in a different timeslot: S_1 in timeslot 1, S_2 in timeslot 2, and R in timeslot 3 (Figure 1). In this paper, we limit the scheme to two sources, but any extension to a larger number of sources is possible by applying the principles explained in the paper. We consider a joint network-channel code over this network, that is, an *overall* codeword $\mathbf{c} = [c_1, \ldots, c_N]^T$ is received at the destination during timeslot 1, timeslot 2, and timeslot 3, which form together one coding block. The codeword is partitioned into three parts: $\mathbf{c}^T = [\mathbf{c}(\mathbf{1})^T \mathbf{c}(\mathbf{2})^T \mathbf{c}(\mathbf{3})^T]$, where $\mathbf{c}(\mathbf{1}) = [c_1, \ldots, c_{N_s}]^T$, $\mathbf{c}(\mathbf{2}) = [c_{N_s+1}, \ldots, c_{2N_s}]^T$, and $\mathbf{c}(\mathbf{3}) = [c_{2N_s+1}, \ldots, c_N]^T$, and where S_1 and S_2 transmit N_s bits (note that each user is given an equal slot length because of fairness), and R transmits N_r bits, so that $N = 2N_s + N_r$. We define the level of cooperation, β, as the ratio N_r/N. Because the users do not communicate between each other, the bits $\mathbf{c}(\mathbf{1})$, transmitted by S_1, and the bits $\mathbf{c}(\mathbf{2})$, transmitted by S_2, are independent.

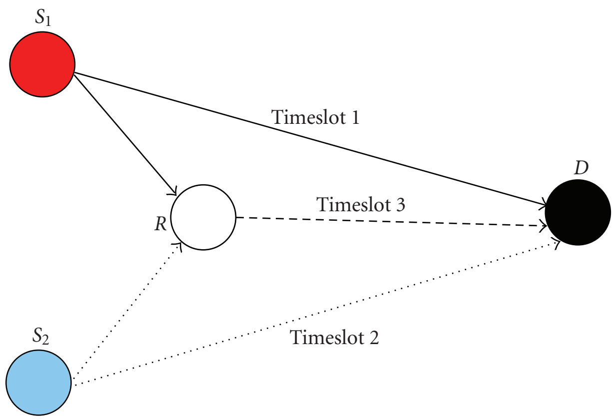

Figure 1: The multiple access relay channel model. The solid arrows correspond to timeslot 1, the dotted arrows to timeslot 2, and the dashed arrow to timeslot 3.

Since the focus in this paper is on coding, BPSK signaling is used for simplicity, so that the transmitters send symbols $x(b)_n \in \{\pm 1\}$, where b stands for the timeslot number and n is the symbol time index in timeslot b. The channel is memoryless with real additive white Gaussian noise and multiplicative real fading. The fading coefficients are only known at the decoder side where the received signal vector at the destination D is

$$\mathbf{y}(b) = \alpha_b \mathbf{x}(b) + \mathbf{w}(b), \quad b = 1, \ldots, 3, \tag{1}$$

where $\mathbf{y}(\mathbf{1}) = [y(1)_1, \ldots, y(1)_{N_s}]^T$, $\mathbf{y}(\mathbf{2}) = [y(2)_1, \ldots, y(2)_{N_s}]^T$, and $\mathbf{y}(\mathbf{3}) = [y(3)_1, \ldots, y(3)_{N_r}]^T$ are the received complex signal vectors in timeslots 1, 2, and 3, respectively. The noise vector $\mathbf{w}(\mathbf{b})$ consists of independent noise samples which are real Gaussian distributed, that is, $w(b)_n \sim \mathcal{N}(0, \sigma^2)$, where $1/2\sigma^2$ is the average signal-to-noise ratio $\gamma = E_s/N_0$. The Rayleigh distributed fading coefficients α_1, α_2 and α_3 are independent and identically distributed. (The average signal-to-noise ratios on the S_1-D, S_2-D; and R-D channels are the same.) The channel model is illustrated in Figure 2. In some parts of the paper, a block binary erasure channel (block BEC) [19, 20] will be assumed, which is a special case of block fading. In a block BEC, the fading gains belong to the set $\{0, \infty\}$, where $\alpha = 0$ means the link is a complete erasure, while $\alpha = \infty$ means the link is perfect.

We assume that no errors occur on the S_1-R and S_2-R channels. This simplifies the analysis and does not change the criteria for the code to attain full-diversity, as will be shown in Section 3.2.

2.2. LDPC Coding. We focus on binary LDPC codes $\mathcal{C}[N, 2K]_2$ with block length N and dimension $2K$, and coding rate $R_c = 2K/N$. (We consider two sources each with K information bits and an overall error-correcting code with N codebits.) The code $\mathcal{C}$ is defined by a parity-check matrix H, or equivalently, by the corresponding Tanner graph [7, 9]. Regular (d_b, d_c) LDPC codes have a parity-check matrix with

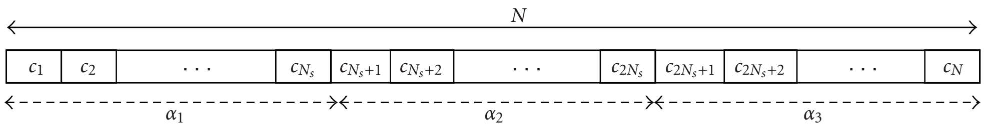

Figure 2: Codeword representation for a multiple access relay channel. The fading gains α_1, α_2, and α_3 are independent.

d_b ones in each column and d_c ones in each row. For irregular $(\lambda(x), \rho(x))$ LDPC codes, these numbers are replaced by the so-called degree distributions [9]. These distributions are the standard polynomials $\lambda(x)$ and $\rho(x)$ [21]:

$$\lambda(x) = \sum_{i=2}^{d_b} \lambda_i x^{i-1}, \qquad \rho(x) = \sum_{i=2}^{d_c} \rho_i x^{i-1}, \tag{2}$$

where λ_i (resp., ρ_i) is the fraction of all edges in the Tanner graph, connected to a bit node (resp., check node) of degree i. Therefore, $\lambda(x)$ and $\rho(x)$ are sometimes referred to as left and right degree distributions from an edge perspective. In Section 6, the polynomials $\mathring{\lambda}(x)$ and $\mathring{\rho}(x)$, which are the left and right distributions from a node perspective, will also be adopted:

$$\mathring{\lambda}(x) = \sum_{i=2}^{d_b} \mathring{\lambda}_i x^{i-1}, \qquad \mathring{\rho}(x) = \sum_{i=2}^{d_c} \mathring{\rho}_i x^{i-1}, \tag{3}$$

where $\mathring{\lambda}_i$ (resp., $\mathring{\rho}_i$) is the fraction of all bit *nodes* (resp., check nodes) in the Tanner graph of degree i, hence $\mathring{\lambda}_i = (\lambda_i/i)/(\sum_j \lambda_j/j)$ and likewise with $\mathring{\rho}_i$.

The goal of this research is to design a full-diversity ensemble of LDPC codes for the MARC. An ensemble of LDPC codes is the set of all LDPC codes that satisfy the left degree distribution $\lambda(x)$ and right degree distribution $\rho(x)$.

In this paper, not all bit nodes and check nodes in the Tanner graph will be treated equally. To elucidate the different classes of bit nodes and check nodes, a compact representation of the Tanner graph, adopted from [22] and also known as protograph representation [9, 23, 24] (and the references therein), will be used. In this compact Tanner graph, bit nodes and check nodes of the same class are merged into one node.

2.3. Physical Layer Network Coding. The coded bits transmitted by R are a linear transformation of the information bits from S_1 and S_2, denoted as $\mathbf{i}(\mathbf{1})$ and $\mathbf{i}(\mathbf{2})$, where both vectors are of length K. (In some papers, the coded bits transmitted by R are a linear transformation of the transmitted bits from S_1 and S_2, which boils down to the same as the information bits, since the transmitted bits (parity bits and information bits) are a linear transformation of the information bits.) Let $*$ stand for a matrix multiplication in GF(5);

$$\mathbf{c}(\mathbf{3}) = T * \begin{bmatrix} \mathbf{i}(\mathbf{1}) \\ \mathbf{i}(\mathbf{2}) \end{bmatrix}. \tag{4}$$

The matrix T represents the *network code*, which has to be designed. Let us split T into two matrices H_N and V such that $T = H_N^{-1} * V$, where H_N is an $N_r \times N_r$ matrix and V is an $N_r \times 2K$ matrix. Now we have the following relation:

$$H_N * \mathbf{c}(\mathbf{3}) = V * \begin{bmatrix} \mathbf{i}(\mathbf{1}) \\ \mathbf{i}(\mathbf{2}) \end{bmatrix}. \tag{5}$$

Equation (5) can be inserted into the parity-check matrix defining the *overall* error-correcting code. Instead of designing T, we can design H_N and V using principles from coding theory.

3. Diversity and Outage Probability of MARC

3.1. Achievable Diversity Order. The formal definition of diversity order on a block fading channel is well known [25].

Definition 1. The diversity order attained by a code $\mathcal{C}$ is defined as

$$d = -\lim_{\gamma \to \infty} \frac{\log P_e}{\log \gamma}, \tag{6}$$

where P_e is the word error rate after decoding.

However, in this document, as far as the diversity order is concerned, we mostly use a block BEC. It has been proved that a coding scheme is of full diversity on the block fading channel if and only if it is of full diversity on a block BEC [22]. The channel model is the same as for block fading, except that the fading gains belong to the set $\{0, \infty\}$. Suppose that on the S_1-D, S_2-D, and R-D links, the probability of a complete erasure, that is, $\alpha = 0$, is ϵ.

Definition 2. A code $\mathcal{C}$ achieves a diversity order d on a block BEC if and only if [26]

$$P_e \propto \epsilon^d, \tag{7}$$

where P_e is the word error rate after decoding and $\propto$ means proportional to.

Therefore, it is sufficient to show that two erased channels cause an error event to prove that $d < 3$, because the probability of this event is proportional to ϵ^2. Consider, for example, that the R-D channel has been erased, as well as the S_1-D channel. Then, the information from S_1 can never reach D, because S_2 does not communicate with S_1. Therefore, the diversity order $d < 3$.

A diversity order of two is achieved if the destination is capable of retrieving the information bits from S_1 and S_2, when exactly one of the S_1-D, S_2-D, or R-D channels is erased. The maximum coding rate allowing the destination to do so will be derived in Section 3.4.

3.2. Perfect Source-Relay Channels. Here, we will show that the achieved diversity at D does not depend on the quality of the source-relay (S-R) channel. Therefore, in the remainder of the paper, we will assume errorless S-R channels to simplify the analysis.

Let us consider a simple block fading relay channel with one source S, one relay R, and one destination D. All considered point-to-point channels (S-R, S-D, R-D) have an intrinsic diversity order of one. In a cooperative protocol, where R has to decode the transmission from S in the first slot, two cases can be distinguished: (1) R is able to decode the transmission from S and cooperates with S in the second slot, hence D receives two messages carrying information from S; (2) R is not able to decode the transmission from S and therefore does not transmit in the second slot, hence D receives only one message carrying information from S, namely, on the S-D channel. Now, the decoding error probability, that is, the WER P_e, at D can be written as follows:

$$P_e = P(\text{case } 1)P(e \mid \text{case } 1) + P(\text{case } 2)P(e \mid \text{case } 2). \tag{8}$$

The probability $P(\text{case } 2)$ is equal to the probability of erroneous decoding at R. For large γ, we have $P(\text{case } 2) \propto 1/\gamma$ and $P(\text{case } 1) = (1 - c/\gamma)$ [25], where c is a constant. The probability $P(e \mid \text{case } 2)$ is equal to the probability of erroneous decoding on the S-D channel; hence for large γ, $P(e \mid \text{case } 2) \propto 1/\gamma$. Now, the error probability P_e at large γ is proportional to

$$P_e \propto P(e \mid \text{case } 1) + \frac{c'}{\gamma^2}, \tag{9}$$

where c' is a positive constant. According to Definition 1, full-diversity requires that at large γ, $P_e \propto 1/\gamma^2$. We see that this only depends on the behavior of $P(e \mid \text{case } 1)$ at large γ, because the second case where the relay cannot decode the transmission from the source in the first slot does automatically give rise to a double diversity order without the need for any code structure. This means that as far as the diversity order is concerned, it is sufficient to assume errorless S-R channels (yielding $P_e = P(e \mid \text{case } 1)$). Furthermore, techniques [8] are known to extend the proposed code construction to nonperfect source-relay channels, so that, for the clarity of the presentation, perfect source-relay channels are assumed in the remainder of the paper.

3.3. Outage Probability of the MARC. We denote an outage event of the MARC by $\mathcal{E}_o$. An outage event is the event that the destination cannot retrieve the information from S_1 or S_2, that is, the transmitted rate is larger than or equal to the instantaneous mutual information. The transmitted rate r_u is the *average* spectral efficiency of user u whereas r is the overall spectral efficiency, so that $r = r_1 + r_2$. (The average spectral efficiency denotes the average number of bits per overall channel uses, including the channel uses of the other devices, that is, transmitted over the MARC channel.) We can interprete r as the total spectral efficiency, that is, transmitted over the network. The MARC block fading channel has a Shannon capacity, that is, essentially zero since the fading gains make the mutual information a random variable which does not allow to achieve an arbitrarily small word error probability under a certain spectral efficiency. This word error probability is called *information outage probability* in the limit of large block length, denoted by

$$P_{\text{out}} = P(\mathcal{E}_o). \tag{10}$$

The outage probability is a lower bound on the average word error rate of coded systems [27].

The mutual information from user 1 to the destination is the weighted sum of the mutual informations from the channels from S_1-D and R-D. (The transmission of R corresponds to redundancy for S_1 and S_2 at the same time. From the point of view of S_1, the transmission of R contains interference from S_2. By using the observations from S_2, the decoder at the destination can at most cancel the interference from S_2 in the transmission from R.) Hence the spectral efficiency r_1 is upper bounded as

$$r_1 < \left(\frac{1-\beta}{2}\right) I(S_1; D) + \beta I(R; D), \tag{11}$$

where $(1 - \beta)/2$ and β are the fractions of the time during which S_1 and R are active [25, Section 5.4.4]. The same holds for user 2:

$$r_2 < \left(\frac{1-\beta}{2}\right) I(S_2; D) + \beta I(R; D). \tag{12}$$

Combining (11) and (12) yields

$$r < \left(\frac{1-\beta}{2}\right) I(S_2; D) + \left(\frac{1-\beta}{2}\right) I(S_1; D) + 2\beta I(R; D). \tag{13}$$

However, there is a tighter bound for r. Indeed, (11) and (12) both rely on the fact that the destination can cancel the interference from the other user on the relay-to-destination channel, but therefore, the destination must be able to decode one of the users' information from their respective transmission. Hence, there exist two scenarios: (1) in the first scenario, D decodes the information of S_2 from the transmission of S_2 ($r_2 < ((1 - \beta)/2)I(S_2; D)$), so that it can cancel the interference from S_2 in the transmission from R ((11) holds); (2) the second scenario is the symmetric case ($r_1 < ((1-\beta)/2)I(S_1; D)$ and (12) holds). Both scenarios lead to a tighter bound for r:

$$r < \left(\frac{1-\beta}{2}\right) I(S_2; D) + \left(\frac{1-\beta}{2}\right) I(S_1; D) + \beta I(R; D). \tag{14}$$

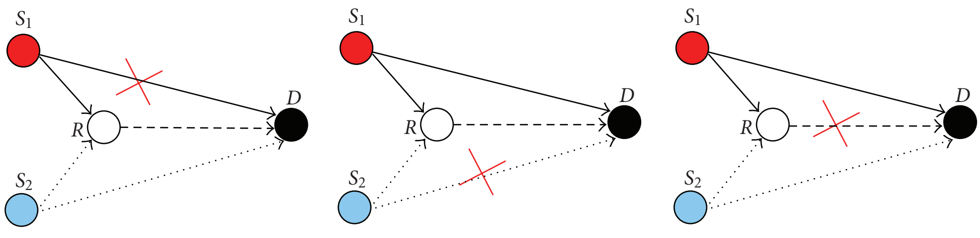

Figure 3: In these three cases, where each time one link is erased, a full-diversity code construction allows the destination to retrieve the information bits from both S_1 and S_2.

Bound (14) can be verified when considering the instantaneous mutual information between the sources and the sinks in the network. We denote the instantaneous mutual information of the MARC as $I(\boldsymbol{\alpha}, \gamma)$, which is a function of the set of fading gains $\boldsymbol{\alpha} = [\alpha_1, \alpha_2, \alpha_3]$ and average SNR γ. The overall mutual information is

$$I(\boldsymbol{\alpha}, \gamma) = \frac{(1-\beta)}{2} I(S_1; D) + \frac{(1-\beta)}{2} I(S_2; D) + \beta I(R; D), \tag{15}$$

because the three timeslots behave as parallel Gaussian channels whose mutual informations add together. Of course, the timeslots timeshare a time-interval, which gives a weight to each mutual information term [25, Section 5.4.4]. The total transmitted rate must be smaller than $I(\boldsymbol{\alpha}, \gamma)$, which yields (14).

From the above analysis, we can now write the expression of an outage event:

$$\begin{aligned}\mathcal{E}_o = \Bigg\{ &\left[r_1 \geq \left(\frac{1-\beta}{2}\right) I(S_1; D) + \beta I(R; D) \right] \\ &\cup \left[r_2 \geq \left(\frac{1-\beta}{2}\right) I(S_2; D) + \beta I(R; D) \right] \\ &\cup \left[r \geq \left(\frac{1-\beta}{2}\right) (I(S_2; D) + I(S_1; D)) + \beta I(R; D) \right] \Bigg\}.\end{aligned} \tag{16}$$

The three terms $I(S_1; D)$, $I(S_2; D)$, and $I(R; D)$ are each the average mutual information of a point-to-point channel with input $x \in \{-1, 1\}$, received signal $y = \alpha x + w$ with $w \sim \mathcal{N}(0, \sigma^2)$, conditioned on the channel realization α, which is determined by the following well-known formula [28]:

$$I(X; Y \mid \alpha) = 1 - \mathbb{E}_{Y|\{x=1,\alpha\}} \left\{ \log_2 \left(1 + \exp\left[\frac{-2y\alpha}{\sigma^2} \right] \right) \right\}, \tag{17}$$

where $\mathbb{E}_{Y|\{x=1,\alpha\}}$ is the mathematical expectation over Y given $x = 1$ and α. Therefore, three terms $I(S_1; D)$, $I(S_2; D)$, and $I(R; D)$ are

$$\begin{aligned} I(S_1; D) &= \mathbb{E}_{Y(1)|\{x(1)=1,\alpha_1\}} \left\{ \log_2 \left(1 + e^{-2y(1)\alpha_1/\sigma^2} \right) \right\}, \\ I(S_2; D) &= \mathbb{E}_{Y(2)|\{x(2)=1,\alpha_2\}} \left\{ \log_2 \left(1 + e^{-2y(2)\alpha_2/\sigma^2} \right) \right\}, \\ I(R; D) &= \mathbb{E}_{Y(3)|\{x(3)=1,\alpha_3\}} \left\{ \log_2 \left(1 + e^{-2y(3)\alpha_3/\sigma^2} \right) \right\}. \end{aligned} \tag{18}$$

Now, the outage probability can be easily determined through Monte-Carlo simulations to average over the fading gains and to average over the noise. (Averaging over the noise can be done more efficiently using Gauss-Hermite quadrature rules [29].)

3.4. Maximum Achievable Coding Rate for Full Diversity. In Section 3.1, we established that the maximum achievable diversity order is two. Here, we will derive an upper bound on the coding rate yielding full diversity, valid for all discrete constellations (assume a discrete constellation with M bits per symbol).

It has been proved that a coding scheme is of full diversity on the block fading channel if and only if it is of full diversity on a block BEC [22]. So let us assume a block BEC, hence $\alpha_i \in \{0, \infty\}$, $i = 1, 2, 3$. The strategy to derive the maximum achievable coding rate is as follows: erase one of the three channels (see Figure 3), and derive the maximum spectral efficiency that allows successful decoding at the destination. (Another approach from a coding point of view has been made in [30].)

The criteria for successful decoding at the destination are given in the previous subsection see (11), (12), and (14). Because one of the three channels has been erased (see Figure 3), one of the mutual informations is zero. The channels that are not erased have a maximum mutual information M (discrete signaling). A user's spectral efficiency allows successful decoding if and only if

$$r_i \leq M \min_{\beta} \left(\left(\frac{1-\beta}{2} \right), \beta \right), \quad i = 1, 2, \tag{19}$$

$$r \leq M \min_{\beta} \left((1-\beta), \frac{1+\beta}{2} \right), \tag{20}$$

It can be easily seen that (20) is a looser bound than (19) ($r = r_1 + r_2$), so that finally

$$r \leq 2M \min_{\beta} \left(\left(\frac{1-\beta}{2} \right), \beta \right), \tag{21}$$

which is maximized if $\beta = 1/3$, such that $r < 2M/3$. The destination decodes all the information bits on one graph that represents an overall code with coding rate R_c. Hence the maximum achievable overall coding rate is $R_c = r/M = 2/3$. It is clear that to maximize $r = r_1 + r_2$, the spectral efficiencies

r_1 and r_2 should be equal, that is, all users in the network transmit at the same rate. In this case, (21) and (19) are equivalent and it is sufficient to bound the sum-rate only. In our design, we will take $r_1 = r_2 = 1/3$, so that the maximum achievable coding rate can be achieved.

4. Full-Diversity Coding for Channels with Multiple Fading States

In the first part of the paper, we established the channel model, the physical layer network coding framework, the maximum achievable diversity order, and the maximum achievable coding rate yielding full diversity. In a nutshell, if the relay transmits a linear transformation of the information bits from both sources during 1/3 of the time, a double diversity order can be achieved with one overall error-correcting code with a maximum coding rate $R_c = 2/3$. Now, in the second part of the paper, this overall LDPC code construction that achieves full diversity for maximum rate will be designed. First, in this section, rootchecks will be introduced, a basic tool to achieve diversity on fading channels under iterative decoding [22]. Then, in the following section, application of these rootchecks to the MARC will define the network code, that is, H_N and V, such that a double-diversity order is achieved. Finally, these claims will be verified by means of simulations for finite length and infinite length codes.

4.1. Diversity Rule. In order to perform close to the outage probability, an error-correcting code must fulfil two criteria:

(1) full-diversity, that is, the slope of the WER is the same as the slope of the outage probability at $\gamma \to \infty$;

(2) coding gain, that is, minimizing the gap between the outage probability and the WER performance at high SNR.

The criteria are given in order of importance. The first criterion is independent of the degree distributions of the code [22], hence serves to construct the skeleton of the code. It guarantees that the gap between the outage probability and the WER performance is not increasing at high SNR. The second criterion can be achieved selecting the appropriate degree distributions or applying the *doping* techniques (see Section 7.2). In this paper, the most attention goes to the first criterion.

In the belief propagation (BP) algorithm, probabilistic messages (log-likelihood ratios) are propagating on the Tanner graph. The behavior of the messages for $\gamma \to \infty$ determines whether the diversity order can be achieved [17]. However, the BP algorithm is numerical and messages propagating on the graph are analytically intractable. Fortunately, there is another much simpler approach to prove full diversity. Diversity is defined at $\gamma \to \infty$. In this region the fading can be modeled by a block BEC, an extremal case of block-Rayleigh fading. Full diversity on the block BEC is a necessary *and sufficient* condition for full diversity on the block-Rayleigh fading channel [22]. The analysis on a block BEC channel is a very simple (bits are erased or perfectly known) but very powerful means to check the diversity order of a system.

Proposition 1. *One obtains a diversity order $d = 2$ on the MARC, provided that all information bits can be recovered, when any single timeslot is erased.*

This rule will be used in the remainder of the paper to derive the skeleton of the code.

4.2. Rootcheck. Applying Proposition 1 to the MARC leads to three possibilities (Figure 3).

Case 1. The S_1-D channel is erased: $\alpha_1 = 0$, $\alpha_2 = \infty$, $\alpha_3 = \infty$

Case 2. The S_2-D channel is erased: $\alpha_1 = \infty$, $\alpha_2 = 0$, $\alpha_3 = \infty$

Case 3. The R-D channel is erased: $\alpha_1 = \infty$, $\alpha_2 = \infty$, $\alpha_3 = 0$.

Let us zoom on the decoding algorithm to see what is happening. We illustrate the decoding procedure on a *decoding tree*, which represents the local neighborhood of a bit node in the Tanner graph (the incoming messages are assumed to be independent). When decoding, bit nodes called *leaves* pass extrinsic information through a check node to another bit node called *root* (Figure 4). Because we consider a block BEC channel, the check node operation becomes very simple. If all leaf bits are known, the root bit becomes the modulo-2 sum of the leaf bits, otherwise, the root bit is undetermined (P(bit=1)=P(bit=0)=0.5). Dealing with Case 3 is simple: let every source send its information uncoded and R sends extra parity bits. If D receives the transmissions of S_1 and S_2 perfectly, it has all the information bits. So the challenging cases are the first two possibilities. Let us assume that the nodes corresponding to the bits transmitted by S_1, S_2, and R are filled red, blue, and white, respectively. Assume that all red (blue) bits are erased at D. A very simple way to guarantee full diversity is to connect a red (blue) information bit node to a *rootcheck* (Figures 4(a) and 4(b)).

Definition 3. A rootcheck is a special type of check node, where all the leaves have colors that are different from the color of its root.

Assigning rootchecks to all the information bits is the key to achieve full diversity. This solution has already been applied in some applications, for example, the cooperative multiple access channel (without external relay) [8]. Note that a check node can be a rootcheck for more than one bit node, for example, the second rootcheck in Figure 4.

4.3. An Example for the MARC. The sources S_1 and S_2 transmit information bits and parity bits that are related to their own information, and R transmits information bits and parity bits related to the information from S_1 and S_2. The previous description naturally leads to 8 different classes of bit nodes. Information bits of S_1 are split into two classes: one class of bits is transmitted on fading gain α_1 (red)

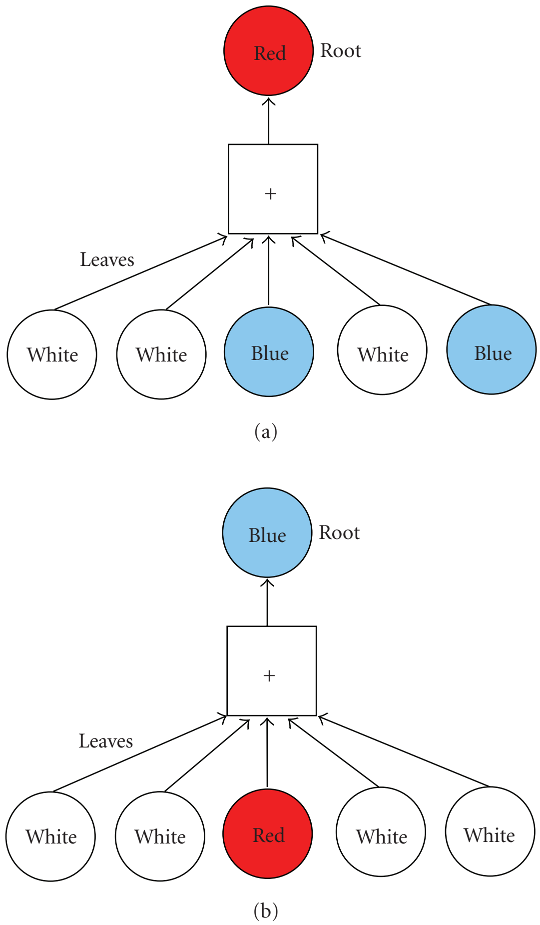

Figure 4: Two examples of a decoding tree, where we distinguish a root and the leaves. While decoding, the leaves pass extrinsic information to the root. Both examples are rootchecks; the root can be recovered if bits corresponding to other *colors* are not erased. (a) recovers the red root bit if all red bits are erased. (b) recovers the blue root bit if all blue bits are erased.

and is denoted as $1i_1$, the other class is transmitted on α_3 (white) and denoted as $2i_1$; similarly, red and white parity bits derived from the message of S_1 are of the classes $1p_1$ and $2p_1$, respectively. Likewise, bits related to S_2 are split into four classes: blue bits $1i_2$ and $1p_2$ (transmitted on α_2), and white bits $2i_2$ and $2p_2$ (transmitted on α_3). The subscripts of a class refer to the associated user. In the remainder of the paper, the vectors $\mathbf{1i_1}$, $\mathbf{2i_1}$, $\mathbf{1p_1}$, and $\mathbf{2p_1}$ collect the bits of the classes $1i_1$, $2i_1$, $1p_1$, and $2p_1$, respectively. A similar notation holds for S_2. This notation is illustrated in Figure 5.

Above, we concluded that all information bits should be the root of a rootcheck. The class of rootchecks for $\mathbf{1i_1}$ is denoted as $1c$. Translating Figure 4 to its matrix representation renders

$$\begin{array}{cccc} \mathbf{1i_1} & \mathbf{1p_1} & \{\mathbf{1i_2}, \mathbf{1p_2}, \mathbf{2i_1}, \mathbf{2p_1}, \mathbf{2i_2}, \mathbf{2p_2}\} & \\ [\mathbf{I} & \mathbf{0} & H_{\text{rest}} &] \quad \mathbf{1c}. \end{array} \tag{22}$$

The identity matrix concatenated with a matrix of zeros assures that bits of the class $1i_1$ are the only red bits connected

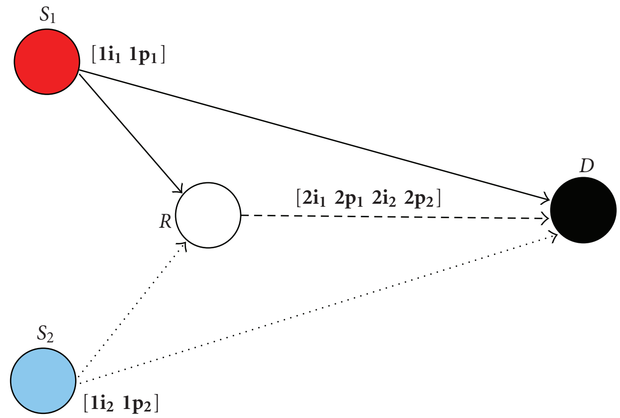

Figure 5: The multiple access relay channel model with the 8 introduced classes of bit nodes.

to check nodes of the class $1c$. (Note that the identity matrix can be replaced by a permutation matrix. For the simplicity of the notation, in the rest of the paper $\mathbf{I}$ will be used.) As the bits from S_1 and S_2 are independent, the matrix representation can be further detailed:

$$\begin{array}{ccccccc} \mathbf{1i_1} & \mathbf{1p_1} & \mathbf{1i_2} & \mathbf{1p_2} & \{\mathbf{2i_1}, \mathbf{2p_1}\} & \mathbf{2i_2} & \mathbf{2p_2} \\ [\mathbf{I} & \mathbf{0} & \mathbf{0} & \mathbf{0} & H'_{\text{rest}} & \mathbf{0} & \mathbf{0}] \quad \mathbf{1c}. \end{array} \tag{23}$$

Hence, a full-diversity code construction for the MARC can be formed by assigning this type of rootchecks (introducing new classes $2c$, $3c$, and $4c$) to all information bits:

$$\begin{array}{c} \begin{array}{cccccccc} \mathbf{1i_1} & \mathbf{1p_1} & \mathbf{1i_2} & \mathbf{1p_2} & \mathbf{2i_1} & \mathbf{2p_1} & \mathbf{2i_2} & \mathbf{2p_2} \end{array} \\ \begin{bmatrix} \mathbf{I} & \mathbf{0} & \mathbf{0} & \mathbf{0} & H_{2i_1} & H_{2p_1} & \mathbf{0} & \mathbf{0} \\ H_{1i_1} & H_{1p_1} & \mathbf{0} & \mathbf{0} & \mathbf{I} & \mathbf{0} & \mathbf{0} & \mathbf{0} \\ \mathbf{0} & \mathbf{0} & \mathbf{I} & \mathbf{0} & \mathbf{0} & \mathbf{0} & H_{2i_2} & H_{2p_2} \\ \mathbf{0} & \mathbf{0} & H_{1i_2} & H_{1p_2} & \mathbf{0} & \mathbf{0} & \mathbf{I} & \mathbf{0} \end{bmatrix} \begin{array}{l} \mathbf{1c} \\ \mathbf{2c} \\ \mathbf{3c} \\ \mathbf{4c}. \end{array} \end{array} \tag{24}$$

(The reader can verify that this is a straightforward extension of full-diversity codes for the block fading channel [22].) S_1 transmits $\mathbf{1i_1}$ and $\mathbf{1p_1}$, S_2 transmits $\mathbf{1i_2}$ and $\mathbf{1p_2}$, and the common relay first transmits $\mathbf{2i_1}$ and $\mathbf{2p_1}$ and then transmits $\mathbf{2i_2}$ and $\mathbf{2p_2}$, hence the level of cooperation is $\beta = 0.5$. The reader can easily verify that if only one color is erased, all information bits can be retrieved after one decoding iteration. Note that both sources do not transmit all information bits, but the relay transmits a part of the information bits. This is possible because if R receives $\mathbf{1i_1}$ and $\mathbf{1p_1}$ perfectly it can derive $\mathbf{2i_1}$ (because of the rootchecks $\mathbf{2c}$) and consequently $\mathbf{2p_1}$ (after reencoding). (This code construction can be easily extended to nonperfect relay channels using techniques described in [8].) The same holds for S_2. It turns out that splitting information bits in two parts and letting one part to be transmitted on the first fading gain and the other part on the second fading gain is the only way to guarantee full diversity for maximum coding rate [22]. This code construction is semirandom, because only parts of the parity-check matrix are randomly generated. However, every set of rows and set of columns contains a randomly generated matrix and, therefore, can conform to any degree distribution. It has been shown that despite the semirandomness (due to the presence of deterministic blocks), these LDPC codes are still very powerful in terms of decoding threshold [22]. No network coding has been used to obtain the code construction discussed above. The aim of this subsection was to show that through rootchecks, it is easy to construct a full-diversity code construction. However, when applying network coding, as will be discussed in Section 5, the spectral efficiency can be increased.

4.4. Rootchecks for Punctured Bits. In the previous subsection, we have illustrated that, through rootchecks, full-diversity can be achieved. Another feature of rootchecks is to retrieve bits that have not been transmitted, which are called punctured bits. Punctured bits are very similar to erased bits, because both are not received by the destination. However, the transmitter knows the exact position of the punctured bits inside the codeword which is not the case for erased bits. Formally, we can state that from an algebraic decoding or a probabilistic decoding point of view, puncturing and erasing are identical, an erased/punctured bit is equivalent to an error with known location but unknown amplitude. From a transmitter point of view, punctured bits have always fixed position in the codeword whereas channel erased bits have random locations.

When punctured bits are information bits, the destination must be able to retrieve them. There are two ways to protect punctured bits.

(i) The punctured bit nodes are connected to one or more rootchecks. If the leaves are erased or punctured, the punctured root bit cannot be retrieved after the first decoding iteration. The erased or punctured leaves on their turn must be connected to rootchecks, such that they can be retrieved after the first iteration. Then, in the second iteration the punctured root bit can be retrieved. These rootchecks are denoted as *second-order rootchecks* (see Figure 6). Similarly, higher-order rootchecks can be used.

(ii) The punctured bit nodes are connected to at least two rootchecks where both rootchecks have leaves with different colors (see Figure 6). If one color is erased, there will always be a rootcheck without erased leaves to retrieve the punctured bit node.

Combinations of both types of rootchecks are also possible.

5. Full-Diversity Joint Network-Channel Code

In this section, we join the principles of the previous section with the physical layer network coding framework. We will use the same bit node classes as in the previous section, hence S_1 transmits $\mathbf{1i_1}$ and $\mathbf{1p_1}$, and S_2 transmits $\mathbf{1i_2}$ and $\mathbf{1p_2}$. The bits transmitted by the relay are determined by (5) and are of the class $c(3)$. Adapting (5) to the classes of bit nodes gives

$$H_N \mathbf{c}(\mathbf{3}) = \begin{bmatrix} V_1 & V_2 & V_3 & V_4 \end{bmatrix} * \begin{bmatrix} \mathbf{1i_1} \\ \mathbf{1i_2} \\ \mathbf{2i_1} \\ \mathbf{2i_2} \end{bmatrix}, \tag{25}$$

where the dimensions of V_i are $N_r \times K/2$. Please note that $\mathbf{2i_1}$, $\mathbf{2p_1}$, $\mathbf{2i_2}$, and $\mathbf{2p_2}$ are not transmitted anymore (these bits are punctured). The number of transmitted bits $\mathbf{c}(\mathbf{3})$ by the relay is determined by the coding rate. There are $2K$ information bits. The sources S_1 and S_2 each transmit K bits, hence to obtain a coding rate $R_c = 2/3$, the relay can transmit $N_r = K$ bits. We will include the punctured information bits $\mathbf{2i_1}$ and $\mathbf{2i_2}$ in the parity-check matrix for two reasons:

(i) without $\mathbf{2i_1}$ and $\mathbf{2i_2}$, we cannot insert (25) in the parity-check matrix;

(ii) the destination wants to recover all information bits, that is, $\mathbf{1i_1}$, $\mathbf{1i_2}$, $\mathbf{2i_1}$, and $\mathbf{2i_2}$, so $\mathbf{2i_1}$ and $\mathbf{2i_2}$ must be included in the decoding graph.

(The matrices in the following of the paper correspond to codewords that must be punctured to obtain the bits actually transmitted.) The parity-check matrix now has the following form:

$$\begin{array}{ccccccc} \mathbf{1i_1} & \mathbf{1p_1} & \mathbf{1i_2} & \mathbf{1p_2} & \mathbf{2i_1} & \mathbf{2i_2} & \mathbf{c(3)} \end{array}$$
$$\left[\begin{array}{ccccccc} H_{1i_1} & H_{1p_1} & \mathbf{0} & \mathbf{0} & \mathbf{I} & \mathbf{0} & \mathbf{0} \\ \mathbf{0} & \mathbf{0} & H_{1i_2} & H_{1p_2} & \mathbf{0} & \mathbf{I} & \mathbf{0} \\ V_1 & \begin{matrix} \mathbf{0} \\ \mathbf{0} \end{matrix} & V_2 & \begin{matrix} \mathbf{0} \\ \mathbf{0} \end{matrix} & V_3 & V_4 & H_N \end{array}\right] \begin{array}{c} \mathbf{1c} \\ \mathbf{2c} \\ \mathbf{3c} \\ \mathbf{4c} \end{array} \tag{26}$$

Because the nodes $\mathbf{2i_1}$ and $\mathbf{2i_2}$ have been added, we have now $4K$ columns and $2K$ rows. K rows are used to implement (25), while the other K rows define $\mathbf{1p_1}$ in terms of the information bits $\mathbf{1i_1}$ and $\mathbf{2i_1}$ (used for encoding at S_1), and $\mathbf{1p_2}$ in terms of the information bits $\mathbf{1i_2}$ and $\mathbf{2i_2}$ (used for encoding at S_2). The first two set of rows $\mathbf{1c}$ and $\mathbf{2c}$ are rootchecks for $\mathbf{2i_1}$ and $\mathbf{2i_2}$; see Section 4. Now it boils down to design the matrices V_1, V_2, V_3, V_4, and H_N, such that the set of rows $\mathbf{3c}$ and $\mathbf{4c}$ represent rootchecks of the first or second order for all information bits. There exist 8 possible parity-check matrices that conform to this requirement; see Appendix A. With the exception of matrix (A.7), all matrices have one or both of the following disadvantages.

(i) There is no random matrix in each set of columns, such that H cannot conform to any degree distribution.

(ii) There is an asymmetry wrt. $\mathbf{2i_1}$ and $\mathbf{2i_2}$ and/or wrt. $\mathbf{1i_1}$ and $\mathbf{1i_2}$ and/or $\mathbf{3c}$ and $\mathbf{4c}$ which results in a loss of coding gain.

Therefore, we select the matrix (A.7). The parity-check matrix (A.7) of the overall decoder at D shows that the bits transmitted by R are a linear transformation of all the information bits $\mathbf{1i_1}$, $\mathbf{2i_1}$, $\mathbf{1i_2}$, and $\mathbf{2i_2}$. Furthermore, the checks $[\mathbf{3c} \quad \mathbf{4c}]$ represent rootchecks for all the information

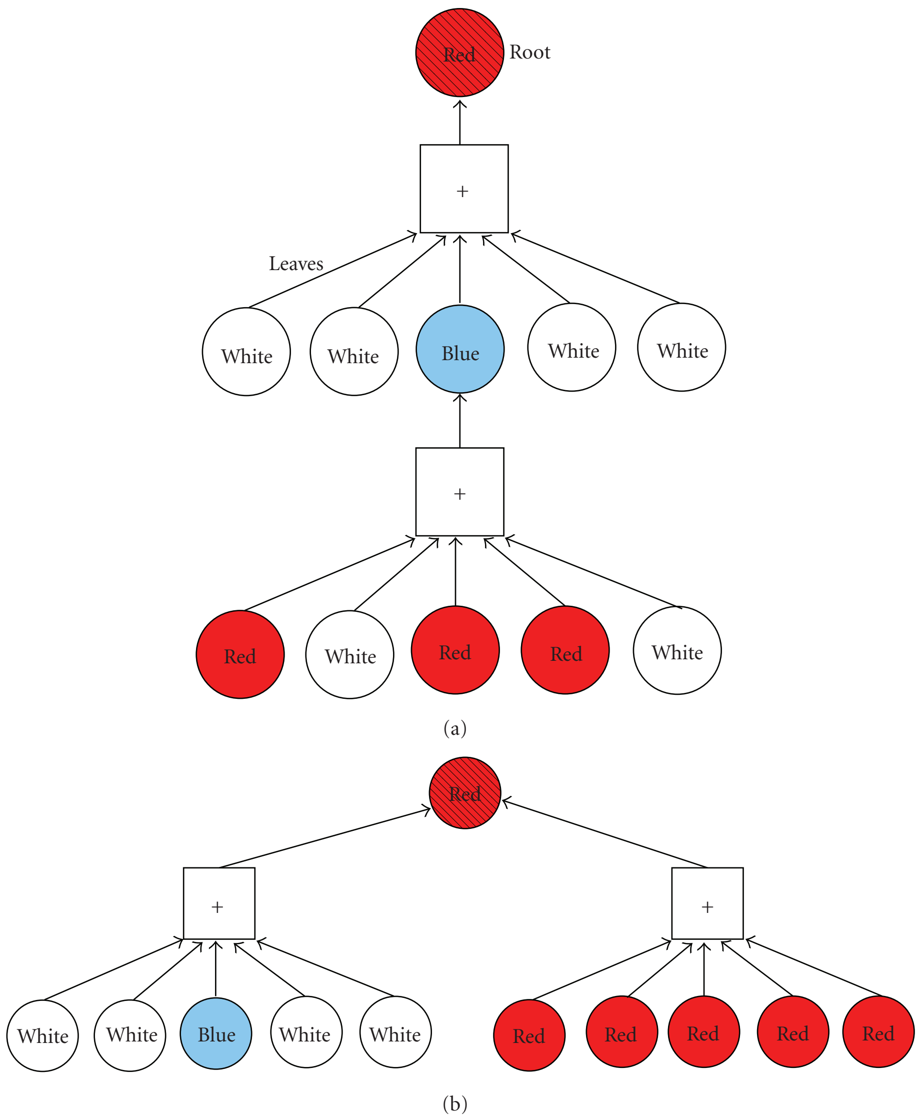

Figure 6: Two special rootchecks for punctured bits (shaded bit nodes). (a) is a second-order rootcheck. Imagine that all blue bits are erased, than the shaded bit node will be retrieved in the second iteration. (b) represents two rootchecks where both rootchecks have leaves with other colors. Imagine that one color has been erased, than the shaded bit node will still be recovered after the first iteration.

bits, guaranteeing full diversity. The checks $[\mathbf{1c} \quad \mathbf{2c}]$ are necessary because the bits $[\mathbf{2i_1} \quad \mathbf{2i_2}]$ are not transmitted. Note that the punctured bits $[\mathbf{2i_1} \quad \mathbf{2i_2}]$ have two rootchecks that have leaves with different colors. One of the rootchecks is a second-order rootcheck. For example, the punctured bits of the class $2i_1$ have two rootchecks, one of the class $1c$ and one of the class $4c$. The rootcheck of the class $1c$ has only red leaves, while the rootcheck of the class $4c$ has white and blue leaves. All but one blue leaves are punctured such that the rootcheck of the class $4c$ is a second-order rootcheck.

6. Density Evolution for the MARC

In this section, we develop the density evolution (DE) framework, to simulate the performance of infinite length LDPC codes. In classical LDPC coding, density evolution [9, 24, 31] is used to simulate the threshold of an ensemble of LDPC codes. (Richardson and Urbanke [9, 31] established that, if the block length is large enough, (almost) all codes in an ensemble of codes behave alike, so the determination of the average behavior is sufficient to characterize a particular code behavior. This average behavior converges to the cycle-free case if the block length augments and it can be found in a deterministic way through density evolution (DE).) The threshold of an ensemble of codes is the minimum SNR at which the bit error rate converges to zero [31].

This technique can also be used to predict the word error rate of an ensemble of LDPC codes [22]. We refer to the event where the bit error probability does not converge to 0 by Density Evolution Outage (DEO). By averaging over a sufficient number of fading instances, we can determine the probability of a Density Evolution Outage P_{DEO}. Now,

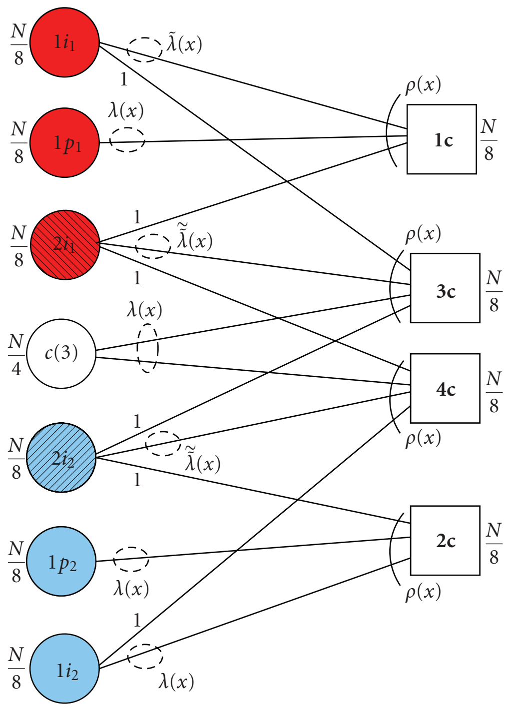

FIGURE 7: A compact representation of the Tanner graph of the proposed code construction (matrix (A.7)), adopted from [22] and also known as protograph representation [23]. Nodes of the same class are merged into one node for the purpose of presentation. Punctured bits are represented by a shaded node.

it is possible to write the word error probability P_e of the ensemble as

$$P_e = P_{e|\text{DEO}} \times P_{\text{DEO}} + P_{e|\text{CONV}} \times (1 - P_{\text{DEO}}), \tag{27}$$

where $P_{e|\text{DEO}}$ is the word error rate given a DEO event and $P_{e|\text{CONV}}$ is the word error rate when DE converges. If the bit error rate does not converge to zero, then the word error rate equals one, so that $P_{e|\text{DEO}} = 1$. On the other hand, $P_{e|\text{CONV}}$ depends on the speed of convergence of density evolution and the population expansion of the ensemble with the number of decoding iterations [32, 33], but in any case $P_e \geq P_{\text{DEO}}$, so that the performance simulated via DE is a lower bound on the word error rate. Finite length simulations confirm the tightness of this lower bound.

In summary, a tight lower bound on the word error rate of infinite length LDPC codes can be obtained by determining the probability of a Density Evolution Outage P_{DEO}. Given a triplet $(\alpha_1, \alpha_2, \alpha_3)$, one needs to track the evolution of message densities under iterative decoding to check whether there is DEO. (Messages are under the form of log-likelihood ratios (LLRs).) The evolution of message densities under iterative decoding is described through the density evolution equations, which are derived directly through the evolution trees. The evolution trees represent the local neighborhood of a bit node in an infinite length code whose graph has no cycles, hence incoming messages to every node are independent.

6.1. Tanner Graph and Notation. The proposed code construction has 7 variable node types and 4 check node types. Consequently, the evolution of message densities under iterative decoding has to be described through multiple evolution trees, which can be derived from the Tanner graph. A Tanner graph is a representation of the parity-check matrices of an error-correcting code. In a Tanner graph, the focus is more on its degree distributions. In Figure 7, the Tanner graph of matrix (A.7) is shown. The new polynomials $\tilde{\lambda}(x)$ and $\tilde{\tilde{\lambda}}(x)$ are derived in Proposition 2.

Proposition 2. *In a Tanner graph with a left degree distribution $\lambda(x)$, isolating one edge per bit node yields a new left degree distribution described by the polynomial $\tilde{\lambda}(x)$:*

$$\tilde{\lambda}(x) = \sum_i \tilde{\lambda}_i x^{i-1}, \qquad \tilde{\lambda}_{i-1} = \frac{\lambda_i (i-1)/i}{\sum_j \lambda_j (j-1)/j}. \tag{28}$$

Proof. Let us define $T_{\text{bit},i}$ as the number of edges connected to a bit node of degree i. Similarly, the number of all edges is denoted T_{bit}. From Section 2, we know that $\lambda(x) = \sum_{i=2}^{d_{b\max}} \lambda_i x^{i-1}$ expresses the left degree distribution, where λ_i is the fraction of all edges in the Tanner graph, connected to a bit node of degree i. So finally $\lambda_i = T_{\text{bit},i}/T_{\text{bit}}$. A similar reasoning can be followed to determine $\tilde{\lambda}_i$:

$$\begin{aligned}\tilde{\lambda}_{i-1} &\overset{(a)}{=} \frac{T_{\text{bit},i} - (\lambda_i/i)T_{\text{bit}}}{T_{\text{bit}} - \sum_j \left(\lambda_j/j\right) T_{\text{bit}}} \\ &\overset{(b)}{=} \frac{\lambda_i T_{\text{bit}} - (\lambda_i/i)T_{\text{bit}}}{T_{\text{bit}} - \sum_j \left(\lambda_j/j\right) T_{\text{bit}}} \\ &= \frac{\lambda_i - \lambda_i/i}{\sum_j \left(\lambda_j/j\right) j - \sum_j \left(\lambda_j/j\right)} \\ &= \frac{(\lambda_i/i)(i-1)}{\sum_j \left(\lambda_j/j\right)(j-1)}.\end{aligned} \tag{29}$$

(a) $\sum_j (\lambda_j/j) T_{\text{bit}}$ is equal to the number of edges that are removed which is equal to the number of bits.

(b) $\lambda_i T_{\text{bit}}$ is equal to the number of edges connected to a bit of degree i. □

Similarly, we can determine $\tilde{\tilde{\lambda}}(x) = \sum_i \tilde{\tilde{\lambda}}_i x^{i-1}$, where $\tilde{\tilde{\lambda}}_{i-2} = (\lambda_i (i-2)/i)/(\sum_j \lambda_j (j-2)/j)$. It can be shown that $\tilde{\tilde{\lambda}}(x)$ is the same as applying the transformation $\tilde{()}$ two times consecutively, hence first on $\lambda(x)$, and then on $\tilde{\lambda}(x)$.

6.2. DE Trees and DE Equations. The proposed code construction has 7 variable node types and 4 check node types. But not all variable node types are connected to all check node types. Therefore, there are 14 evolution trees. But it is sufficient to draw only 7 of them because of symmetry. To write down the equations we adopt the following notation.

Let $X_1 \sim p_1(x)$ and $X_2 \sim p_2(x)$ be two independent real random variables. The density function of X_1+X_2 is obtained by convolving the two original densities, written as $p_1(x) \otimes p_2(x)$. The notation $p(x)^{\otimes n}$ denotes the convolution of $p(x)$ with itself n times.

The density function $p(y)$ of the variable $Y = 2\text{th}^{-1}(\text{th}(X_1/2)\text{th}(X_2/2))$, obtained through a check node with X_1 and X_2 at the input, is obtained through the *R-convolution* [9], written as $p_1(x) \odot p_2(x)$. The notation $\text{th}(\cdot)$ denotes the tangent hyperbolic function and $p(x)^{\odot n}$ denotes the *R*-convolution of $p(x)$ with itself n times.

To simplify the notations, we use the following definitions:

$$\lambda(p(x)) = \sum_i \lambda_i p(x)^{\otimes i-1}, \qquad \rho(p(x)) = \sum_i \rho_i p(x)^{\odot i-1}. \tag{30}$$

Next, we will use the following definitions:

$$\begin{aligned} \rho(p(x), t(x)) &= \sum_i \left(\rho_i p(x)^{\odot i-1} \odot t(x)\right), \\ \lambda^*(p(x)) &= \sum_i \lambda_i p(x)^{\otimes i-2}, \\ \rho^*(p(x)) &= \sum_i \rho_i p(x)^{\odot i-2}. \end{aligned} \tag{31}$$

The first definition is necessary because of the nonlinearity of the R-convolution. Therefore, the first equation is not equal to $t(x) \odot \rho(p(x))$.

The following message densities at the mth iteration are distinguished:

$$\begin{aligned} a_1^m(x)(x) &= \text{density of message from } 1i_1 \text{ to } 1c, \\ f_1^m(x) &= \text{density of message from } 1i_1 \text{ to } 3c, \\ k_1^m(x) &= \text{density of message from } 1p_1 \text{ to } 1c, \\ l_1^m(x) &= \text{density of message from } 2i_1 \text{ to } 1c, \\ q_1^m(x) &= \text{density of message from } 2i_1 \text{ to } 3c, \\ g_2^m(x) &= \text{density of message from } 2i_2 \text{ to } 3c, \\ b_1^m(x) &= \text{density of message from } c(3) \text{ to } 3c, \\ \mu_1(x) &= \text{density of the likelihood of the channel in the} \\ &\qquad \text{1st timeslot.} \end{aligned} \tag{32}$$

Proposition 3. *The DE equations in the neighborhood of* $1i_1$, $1p_1$, $2i_1$, *and* $c(3)$ *for all* m *are listed in* (33)–(34),

$$\begin{aligned} a_1^{m+1}(x) &= \mu_1(x) \otimes \tilde{\lambda}\left(\tilde{\rho}\left(f_{1i1c}a_1^m(x) + f_{1p1c}k_1^m(x), l_1^m(x)\right)\right) \\ &\quad \otimes \mathring{\rho}^*\left(f_{2i3c}q_1^m(x) + f_{c(3)3c}b_1^m(x), g_2^m(x)\right), \\ f_1^{m+1}(x) &= \mu_1(x) \otimes \mathring{\lambda}\left(\tilde{\rho}\left(f_{1i1c}a_1^m(x) + f_{1p1c}k_1^m(x), l_1^m(x)\right)\right), \\ k_1^{m+1}(x) &= \mu_1(x) \otimes \lambda\left(\tilde{\rho}\left(f_{1i1c}a_1^m(x) + f_{1p1c}k_1^m(x), l_1^m(x)\right)\right), \\ l_1^{m+1}(x) &= \mathring{\lambda}^*\left(\tilde{\tilde{\rho}}\left(f_{2i3c}q_1^m(x) + f_{c(3)3c}b_1^m(x), f_1^m(x), g_2^m(x)\right)\right) \\ &\quad \otimes \mathring{\rho}^*\left(f_{2i4c}q_2^m(x) + f_{c(3)4c}b_2^m(x), f_2^m(x)\right), \\ q_1^{m+1}(x) &= \tilde{\tilde{\lambda}}\left(\tilde{\tilde{\rho}}\left(f_{2i3c}q_1^m(x) + f_{c(3)3c}b_1^m(x), f_1^m(x), g_2^m(x)\right)\right) \\ &\quad \otimes \mathring{\rho}\left(f_{1i1c}a_1^m(x) + f_{1p1c}k_1^m(x)\right) \\ &\quad \otimes \rho^*\left(f_{2i4c}q_2^m(x) + f_{c(3)4c}b_2^m(x), f_2^m(x)\right), \\ g_1^{m+1}(x) &= \mathring{\lambda}^*\left(\tilde{\tilde{\rho}}\left(f_{2i3c}q_1^m(x) + f_{c(3)3c}b_1^m(x), f_1^m(x), g_2^m(x)\right)\right) \\ &\quad \otimes \mathring{\rho}\left(f_{1i1c}a_1^m(x) + f_{1p1c}k_1^m(x)\right), \end{aligned} \tag{33}$$

$$\begin{aligned} b_1^{m+1}(x) = \mu_3(x) \otimes \lambda\Big(f_{3cc(3)} \cdot \tilde{\tilde{\rho}}\big(f_{2i3c}q_1^m(x) &+ f_{c(3)3c} \\ \cdot b_1^m(x), f_1^m(x), g_2^m(x)\big) &+ f_{4cc(3)} \\ \times \tilde{\tilde{\rho}}\big(f_{2i4c}q_2^m(x) &+ f_{c(3)4c}b_2^m(x), \\ f_2^m(x), g_1^m(x)\big)\Big), \end{aligned} \tag{34}$$

where

$$f_{1i1c} = \frac{\sum_i \mathring{\lambda}_i(i-1)}{\sum_i \mathring{\rho}_i(i-1)}, \tag{35}$$

$$f_{1p1c} = 1 - f_{1i1c} = \frac{\sum_i \mathring{\lambda}_i i}{\sum_i \mathring{\rho}_i(i-1)}, \tag{36}$$

$$f_{2i3c} = \frac{\sum_i \mathring{\lambda}_i(i-2)}{\sum_i \mathring{\rho}_i(i-2)}, \tag{37}$$

$$f_{c(3)3c} = 1 - f_{2i3c} = \frac{\sum_i \mathring{\lambda}_i i}{\sum_i \mathring{\rho}_i(i-2)}, \tag{38}$$

$$f_{2i4c} = f_{2i3c}, \tag{39}$$

$$f_{c(3)4c} = f_{c(3)3c}, \tag{40}$$

$$f_{3cc(3)} = 1 - f_{4cc(3)}, \tag{41}$$

$$f_{3cc(3)} = 0.5 * \frac{f_{c(3)3c}\sum_i \mathring{\rho}_i(i-2)}{\sum_i \mathring{\lambda}_i(i)}, \tag{42}$$

$$f_{4cc(3)} = 0.5 * \frac{f_{c(3)4c}\sum_i \mathring{\rho}_i(i-2)}{\sum_i \mathring{\lambda}_i(i)}, \tag{43}$$

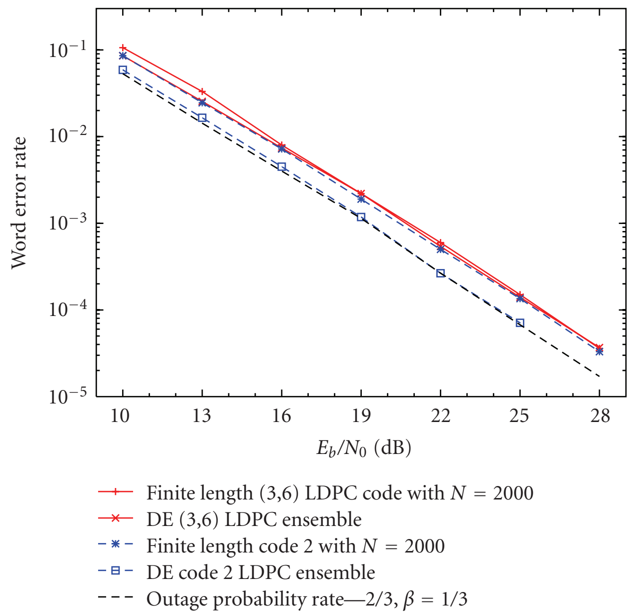

Figure 8: Density evolution of full-diversity LDPC ensembles with maximum coding rate $R_c = 2/3$ with iterative decoding on a MARC. E_b/N_0 is the average information bit energy-to-noise ratio on the S_1-D, S_2-D, and R-D links.

Note that the message densities propagating from bits of the class $2i_1$ do not contain a channel observation $\mu_1(x)$ because these information bits are punctured.

Proof. See Appendix B. □

7. Numerical Results

7.1. Full-Diversity LDPC Ensembles. We evaluated the finite length performance of full-diversity LDPC codes and the asymptotic performance by applying DE on the proposed code construction. The parity-check matrix (A.7) is used by the destination to decode the information bits. This paper focuses on full diversity, rather than coding gain. Therefore, one of the codes is a simple regular (3, 6) LDPC code. This means that all the random matrices in (A.7) are randomly generated satisfying an overall row weight of 6 and an overall column weight of 3. This matrix corresponds to a coding rate of 0.5, but because $[\mathbf{2i_1} \quad \mathbf{2i_2}]$ are punctured, the actual coding rate is $R_c = 2/3$. The other code, that is, simulated and is denoted as *code 2* is an irregular $(\lambda(x), \rho(x))$ LDPC ensemble [22] with left and right degree distributions given by the polynomials

$$\lambda(x) = 0.285486x + 0.31385x^2 + 0.199606x^7 + 0.201058x^{14},$$
$$\rho(x) = x^8. \tag{44}$$

We studied the following scenario.

(i) The S_1-D, S_2-D, and R-D links have the same average SNR.

(ii) The S_1-R and S_2-R links are perfect.

(iii) The coding rate is $R_c = 2/3$ and the cooperation level is $\beta = 2/3$.

Figure 8 shows the main results: the word error rate (WER) of a regular (3, 6) LDPC ensemble and of an irregular $(\lambda(x), \rho(x))$ LDPC ensemble, which are both of full diversity.

It is clear that the DE results are a lower bound on the actual word error rates (a tight lower bound for the regular code and a less tight lower bound for the irregular code). The word error rate of a regular (3, 6) LDPC code is only about 1.5 dB worse than the outage probability. The irregular LDPC code is only slightly better than the regular (3, 6) LDPC code in terms of word error rate.

7.2. Full-Diversity RA Codes with Improved Coding Gain. Another technique, suggested in [17], that improves the coding gain is called *doping*. For all the Rootcheck based LDPC codes the reliability of the messages exchanged by the belief propagation algorithm can be improved by increasing the reliability of parity bits (which are not protected by rootchecks). In fact the LLR values of the messages exchanged by the belief propagation algorithm are in the form [17]:

$$\Lambda_l^m \propto \sum_{i=1}^{B} a_i \alpha_i^2 + \eta, \tag{45}$$

where α_i are the fading coefficients, a_i are positive constants, and η represents the noise. The higher the coefficients a_i, the more reliable are the LLR messages. Since the output messages of the check node are limited by the lowest LLR values of the incoming messages, that is, the messages coming from parity bits, the doping technique aims to increase those values. The least reliable variable nodes are the parity bits sent on a channel in a deep fade.

In case of block BEC, consider the parity bits sent on a channel with fading coefficient $\alpha_1 = 0$ and suppose that all the other fading coefficients are $\alpha_i = \infty$ with $i \neq 1$. Consider the parity-check matrix (A.7). The doping technique consists in fixing the random matrix H_{1p_1} such that, under BP, all the variable nodes can be recovered after a certain number of iterations. This is equivalent to having reliable parity bits, that is, connected to rootchecks of a certain order, and it guarantees to increase the coefficients a_i.

While the aforementioned doping technique has been proposed and investigated for infinite length LDPC codes, finite length rootcheck based LDPC codes that get advantage of the doping technique have not been published yet. Ongoing studies have revealed construction problems with doped finite length Root-LDPC codes, so that their performance cannot be included here. An important issue, that is often not considered, is the encoding complexity. This suggests to embed the well-known repeat-accumulate (RA) structure in the parity-check matrix, which results in linear-time encoding. Hence, regardless the degree distribution, we

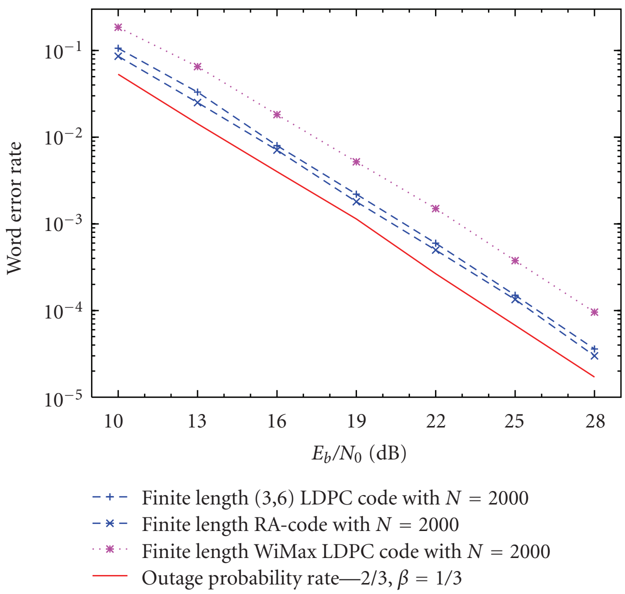

FIGURE 9: Comparison of proposed code construction with results from literature. E_b/N_0 is the average information bit energy-to-noise ratio on the S_1-D, S_2-D, and R-D links.

substitute the matrices H_{1p_1}, H_{1p_2}, and H_N with staircase matrices (46)

$$\begin{bmatrix} 1 & 0 & 0 & \cdots & 0 \\ 1 & 1 & 0 & \cdots & 0 \\ 0 & 1 & 1 & \cdots & 0 \\ \vdots & & \ddots & \ddots & \vdots \\ 0 & 0 & \cdots & 1 & 1 \end{bmatrix}. \tag{46}$$

Figure 9 reports the simulation results for a regular RA code that show a 0.5 dB improvement compared to the proposed regular (3,6) code. Together with the fact that this simple code is now linear-time encoding, this result is impressive because we have lowered the complexity and improved the performance at the same time. As a benchmark the outage probability has been plotted. We have also included the best known LDPC code for the MARC in literature: the rate 2/3 network code proposed in [16]; it reports a loss of almost 2.5 dB wrt. the proposed full-diversity RA code.

8. Conclusions and Remarks

We have studied LDPC codes for the multiple access relay channel in a slowly varying fading environment under iterative decoding. LDPC codes must be carefully designed to achieve full diversity on this channel and network coding must be applied to increase the achievable coding rate to a maximum rate $R_{c\max} = 2/3$. Combining network coding with of full diversity channel coding gave rise to a new family of semirandom full-diversity joint network-channel LDPC codes for all rates not exceeding $R_{c\max} = 2/3$. A code that is only 1.5 dB away from the outage probability limit has been presented.

For a block fading channel with several fading states per codeword, it has been pointed out that the poor reliability of the parity bits in full-diversity LDPC codes (where especially the information bits are well protected) causes the actual gap with the outage probability limit. We increased the reliability of the parity bits by using a repeat-accumulate structure and have improved the coding gain of the presented code construction for the MARC.

Appendices

A. Full-Diversity Parity-Check Matrices

The reader can find here a list of full-diversity parity-check matrices H, that is, matrices where all information bits are assigned to a rootcheck in the last two set of rows **3c** and **4c**. Matrix (A.7) performs the best for reasons of symmetry and randomness,

$$\begin{array}{ccccccc|c} 1i_1 & 1p_1 & 1i_2 & 1p_2 & 2i_1 & 2i_2 & c(3) & \\ H_{1i_1} & H_{1p_1} & \mathbf{0} & \mathbf{0} & \mathbf{I} & \mathbf{0} & \mathbf{0} & \mathbf{1c} \\ \mathbf{0} & \mathbf{0} & H_{1i_2} & H_{1p_2} & \mathbf{0} & \mathbf{I} & \mathbf{0} & \mathbf{2c} \\ \mathbf{I} & \mathbf{0} & \mathbf{I} & \mathbf{0} & H_{2i_1} & \mathbf{0} & H_N & \mathbf{3c} \\ \mathbf{0} & \mathbf{0} & H_{2i_2} & \mathbf{0} & \mathbf{I} & \mathbf{I} & & \mathbf{4c} \end{array} \tag{A.1}$$

$$\begin{array}{ccccccc|c} 1i_1 & 1p_1 & 1i_2 & 1p_2 & 2i_1 & 2i_2 & c(3) & \\ H_{1i_1} & H_{1p_1} & \mathbf{0} & \mathbf{0} & \mathbf{I} & \mathbf{0} & \mathbf{0} & \mathbf{1c} \\ \mathbf{0} & \mathbf{0} & H_{1i_2} & H_{1p_2} & \mathbf{0} & \mathbf{I} & \mathbf{0} & \mathbf{2c} \\ \mathbf{I} & \mathbf{0} & \mathbf{I} & \mathbf{0} & H_{2i_1} & H_{2i_2} & H_N & \mathbf{3c} \\ \mathbf{0} & \mathbf{0} & \mathbf{0} & \mathbf{0} & \mathbf{I} & \mathbf{I} & & \mathbf{4c} \end{array} \tag{A.2}$$

$$\begin{array}{ccccccc|c} 1i_1 & 1p_1 & 1i_2 & 1p_2 & 2i_1 & 2i_2 & c(3) & \\ H_{1i_1} & H_{1p_1} & \mathbf{0} & \mathbf{0} & \mathbf{I} & \mathbf{0} & \mathbf{0} & \mathbf{1c} \\ \mathbf{0} & \mathbf{0} & H_{1i_2} & H_{1p_2} & \mathbf{0} & \mathbf{I} & \mathbf{0} & \mathbf{2c} \\ \mathbf{I} & \mathbf{0} & \mathbf{I} & \mathbf{0} & \mathbf{0} & H_{2i_1} & H_N & \mathbf{3c} \\ H_{2i_2} & \mathbf{0} & \mathbf{0} & \mathbf{0} & \mathbf{I} & \mathbf{I} & & \mathbf{4c} \end{array} \tag{A.3}$$

$$\begin{array}{ccccccc|c} 1i_1 & 1p_1 & 1i_2 & 1p_2 & 2i_1 & 2i_2 & c(3) & \\ H_{1i_1} & H_{1p_1} & \mathbf{0} & \mathbf{0} & \mathbf{I} & \mathbf{0} & \mathbf{0} & \mathbf{1c} \\ \mathbf{0} & \mathbf{0} & H_{1i_2} & H_{1p_2} & \mathbf{0} & \mathbf{I} & \mathbf{0} & \mathbf{2c} \\ \mathbf{I} & \mathbf{0} & \mathbf{I} & \mathbf{0} & \mathbf{0} & \mathbf{0} & H_N & \mathbf{3c} \\ H_{2i_1} & \mathbf{0} & H_{2i_2} & \mathbf{0} & \mathbf{I} & \mathbf{I} & & \mathbf{4c} \end{array} \tag{A.4}$$

$$\begin{array}{ccccccc|c} 1i_1 & 1p_1 & 1i_2 & 1p_2 & 2i_1 & 2i_2 & c(3) & \\ H_{1i_1} & H_{1p_1} & \mathbf{0} & \mathbf{0} & \mathbf{I} & \mathbf{0} & \mathbf{0} & \mathbf{1c} \\ \mathbf{0} & \mathbf{0} & H_{1i_2} & H_{1p_2} & \mathbf{0} & \mathbf{I} & \mathbf{0} & \mathbf{2c} \\ \mathbf{I} & \mathbf{0} & H_{2i_1} & \mathbf{0} & \mathbf{0} & \mathbf{I} & H_N & \mathbf{3c} \\ H_{2i_2} & \mathbf{0} & \mathbf{I} & \mathbf{0} & \mathbf{I} & \mathbf{0} & & \mathbf{4c} \end{array} \tag{A.5}$$

$$\begin{array}{ccccccc|c} 1i_1 & 1p_1 & 1i_2 & 1p_2 & 2i_1 & 2i_2 & c(3) & \\ H_{1i_1} & H_{1p_1} & \mathbf{0} & \mathbf{0} & \mathbf{I} & \mathbf{0} & \mathbf{0} & \mathbf{1c} \\ \mathbf{0} & \mathbf{0} & H_{1i_2} & H_{1p_2} & \mathbf{0} & \mathbf{I} & \mathbf{0} & \mathbf{2c} \\ \mathbf{I} & \mathbf{0} & H_{2i_1} & \mathbf{0} & H_{2i_2} & \mathbf{I} & H_N & \mathbf{3c} \\ \mathbf{0} & \mathbf{0} & \mathbf{I} & \mathbf{0} & \mathbf{I} & \mathbf{0} & & \mathbf{4c} \end{array} \tag{A.6}$$

$$\begin{array}{c} \begin{matrix} 1i_1 & 1p_1 & 1i_2 & 1p_2 & 2i_1 & 2i_2 & c(3) \end{matrix} \\ \left[\begin{matrix} H_{1i_1} & H_{1p_1} & \mathbf{0} & \mathbf{0} & \mathbf{I} & \mathbf{0} & \mathbf{0} \\ \mathbf{0} & \mathbf{0} & H_{1i_2} & H_{1p_2} & \mathbf{0} & \mathbf{I} & \mathbf{0} \\ \mathbf{I} & \mathbf{0} & \mathbf{0} & \mathbf{0} & H_{2i_1} & \mathbf{I} & \\ \mathbf{0} & \mathbf{0} & \mathbf{I} & \mathbf{0} & \mathbf{I} & H_{2i_2} & H_N \end{matrix}\right] \begin{matrix} \mathbf{1c} \\ \mathbf{2c} \\ \mathbf{3c} \\ \mathbf{4c} \end{matrix} \end{array} \quad \text{(A.7)}$$

$$\begin{array}{c} \begin{matrix} 1i_1 & 1p_1 & 1i_2 & 1p_2 & 2i_1 & 2i_2 & c(3) \end{matrix} \\ \left[\begin{matrix} H_{1i_1} & H_{1p_1} & \mathbf{0} & \mathbf{0} & \mathbf{I} & \mathbf{0} & \mathbf{0} \\ \mathbf{0} & \mathbf{0} & H_{1i_2} & H_{1p_2} & \mathbf{0} & \mathbf{I} & \mathbf{0} \\ \mathbf{I} & \mathbf{0} & \mathbf{0} & \mathbf{0} & \mathbf{0} & \mathbf{I} & \\ H_{2i_1} & \mathbf{0} & \mathbf{I} & \mathbf{0} & \mathbf{I} & H_{2i_2} & H_N \end{matrix}\right] \begin{matrix} \mathbf{1c} \\ \mathbf{2c} \\ \mathbf{3c} \\ \mathbf{4c} \end{matrix} \end{array} \quad \text{(A.8)}$$

B. Proof of Proposition 3

Equations (33)–(40) are directly derived from the local neighborhood trees (see e.g., Figures 11 and 12). The proportionality factors (35)–(40) can easily be determined by analyzing the Tanner graph. Let T denote the total number of edges between the variable nodes ($\mathbf{1i_1} - \mathbf{1p_1}$) and the check nodes $\mathbf{1c}$. Figure 10 illustrates how f_{1p1c} and f_{1i1c} are obtained:

$$T \overset{(a)}{=} \frac{N}{8}\sum_i \mathring{\rho}_i (i-1), \quad \text{(B.1)}$$

$$T_{1p} \overset{(a)}{=} \frac{N}{8}\sum_i \mathring{\lambda}_i i, \qquad T_{1i} \overset{(a)}{=} \frac{N}{8}\sum_i \mathring{\lambda}_i (i-1), \quad \text{(B.2)}$$

$$f_{1p1c} \overset{(b)}{=} \frac{T_{1p}}{T}, \qquad f_{1i1c} \overset{(b)}{=} \frac{T_{1i}}{T}. \quad \text{(B.3)}$$

(a) The fraction of check nodes connected to $(i-1)$ edges of T is $\mathring{\rho}_i(N/8)$. A similar reasoning proves (B.2).

(b) The fraction of edges T connecting $\mathbf{1p_1}$ to $\mathbf{1c}$ is f_{1p1c} and the fraction of edges T connecting $\mathbf{1i_1}$ to $\mathbf{1c}$ is f_{1i4c}.

Note that in the first iteration, $a_1^1(x)$, $f_1^1(x)$, $k_1^1(x)$, and $b_1^1(x)$ are equal to $\mu_1(x)$, because the received messages come from check nodes where one of the leaves corresponds to a punctured information bit (so that their message density is a Dirac function on LLR $= 0$). Therefore, the message densities coming from the check nodes are also Dirac functions on LLR $= 0$. (The output of a check node y is determined through its inputs x_i, $i = 1 \cdots d_c - 1$ via the following formula: $\text{th}(y/2) = \prod_{i=1}^{d_c-1}\text{th}(x_i/2)$. If one of the inputs x_i is always zero because its distribution is a Dirac function on LLR $= 0$, then the output y will always be zero, so that its distribution will also be a Dirac function on LLR $= 0$.) But $q_1(x)$ and $g_1(x)$ are different from a Dirac function on LLR $= 0$ after the first iteration, so that the next iteration also $l_1(x)$ becomes different from a Dirac function on LLR $= 0$.

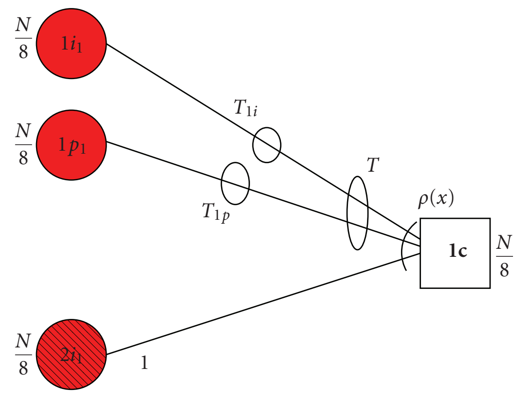

FIGURE 10: Part of the compact graph representation of the Tanner graph of proposed code construction. The number of edges connecting $(1i_1 - 1p_1)$ to $\mathbf{1c}$ is T. The number of edges connecting $1p_1$ to $\mathbf{1c}$ is T_{1p}. The number of edges connecting $1i_1$ to $\mathbf{1c}$ is T_{1i}.

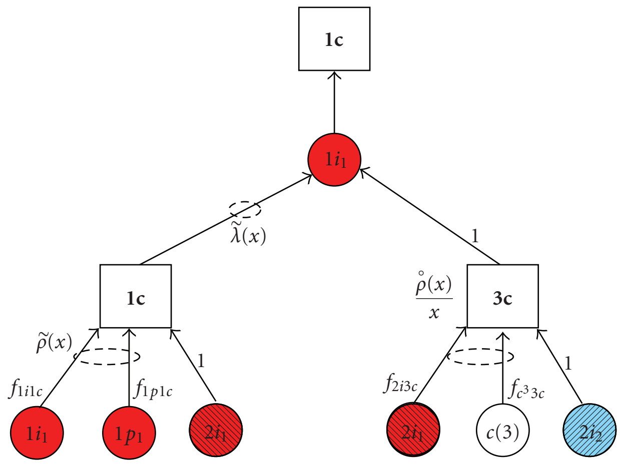

FIGURE 11: Local neighborhood of a bit node of the class $1i_1$. This tree is used to determine $a_1^{m+1}(x)$.

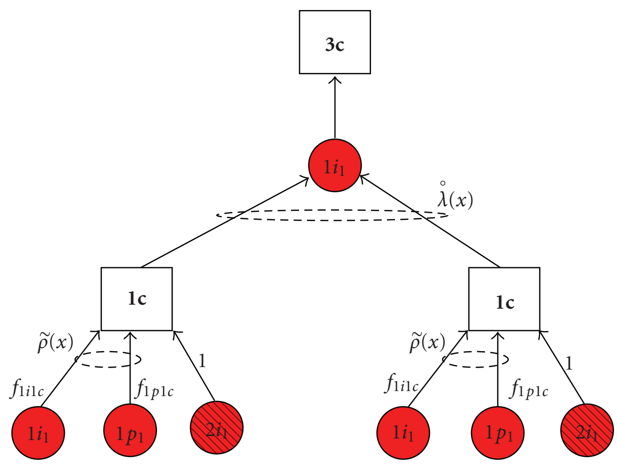

FIGURE 12: Local neighborhood of a bit node of the class $1i_1$. This tree is used to determine $f_1^{m+1}(x)$.

The factor 0.5 in (42) and (43) takes into account that $c(3)$ counts $N/4$ variable nodes while $3c$ and $4c$ count only $N/8$ parity check equations. Solving together (40)–(43), it is possible to prove that for any degree distribution

$$f_{3cc(3)} = f_{4cc(3)} = \frac{1}{2}. \tag{B.4}$$

Acknowledgments

D. Capirone wants to acknowledge professor Benedetto for helpful and stimulating discussions. This work was supported by the European Commission in the framework of the FP7 Network of Excellence in Wireless COMmunications NEWCOM++ (Contract no. 216715).

References

[1] A. Sendonaris, E. Erkip, and B. Aazhang, "User cooperation diversity—part I: system description," *IEEE Transactions on Communications*, vol. 51, no. 11, pp. 1927–1938, 2003.

[2] A. Sendonaris, E. Erkip, and B. Aazhang, "User cooperation diversity—part II: implementation aspects and performance analysis," *IEEE Transactions on Communications*, vol. 51, no. 11, pp. 1939–1948, 2003.

[3] J. N. Laneman, D. N. C. Tse, and G. W. Wornell, "Cooperative diversity in wireless networks: efficient protocols and outage behavior," *IEEE Transactions on Information Theory*, vol. 50, no. 12, pp. 3062–3080, 2004.

[4] T. Hunter, *Coded cooperation: a new framework for user cooperation in wireless systems*, Ph.D. dissertation, University of Texas at Dallas, Richardson, Tex, USA, 2004.

[5] E. Van Der Meulen, "Three-terminal communication channels," *Advances in Applied Probability*, vol. 3, no. 1, pp. 120–154, 1971.

[6] T. M. Cover and A. A. Gamal, "Capacity theorems for the relay channel," *IEEE Transactions on Information Theory*, vol. 25, no. 5, pp. 572–584, 1979.

[7] E. Biglieri, *Coding for the Wireless Channel*, Springer, New York, NY, USA, 2005.

[8] D. Duyck, J. Boutros, and M. Moeneclaey, "Low-density graph codes for slow fading relay channels," *IEEE Transactions on Information Theory*, http://telin.ugent.be/~dduyck/publications/paper_ldpc_cooperative.pdf. In press.

[9] T. Richardson and R. Urbanke, *Modern Coding Theory*, Cambridge University Press, Cambridge, UK, 2008.

[10] J. Boutros, G. I. Fàbregas, and E. Calvanese-Strinati, "Analysis of coding on non-ergodic channels," in *Proceedings of the Allerton Conference on Communication, Control and Computing*, 2005.

[11] R. Knopp and P. A. Humblet, "On coding for block fading channels," *IEEE Transactions on Information Theory*, vol. 46, no. 1, pp. 189–205, 2000.

[12] C. Hausl, *Joint network-channel coding for wireless relay networks*, Ph.D. dissertation, Technische Universität München, München, Germany, November 2008.

[13] R. Ahlswede, N. Cai, S.-Y. R. Li, and R. W. Yeung, "Network information flow," *IEEE Transactions on Information Theory*, vol. 46, no. 4, pp. 1204–1216, 2000.

[14] C. Hausl and P. Dupraz, "Joint network-channel coding for the multiple-access relay channel," in *Proceedings of the 3rd Annual IEEE Communications Society on Sensor and Ad Hoc Communications and Networks (Secon '06)*, vol. 3, pp. 817–822, September 2006.

[15] C. Hausl, F. Schreckenbach, I. Oikonomidis, and G. Bauch, "Iterative network and channel decoding on a tanner graph," in *Proceedings of the Allerton Conference on Communication, Control and Computing*, 2005.

[16] L. Chebli, C. Hausl, G. Zeitler, and R. Koetter, "Cooperative uplink of two mobile stations with network coding based on the WiMax LDPC code," in *Proceedings of the IEEE Global Telecommunications Conference (GLOBECOM '09)*, 2009.

[17] J. J. Boutros, "Diversity and coding gain evolution in graph codes," in *Proceedings of the Information Theory and Applications Workshop (ITA '09)*, pp. 34–43, February 2009.

[18] D. Capirone, D. Duyck, and M. Moeneclaey, "Repeat-accumulate and Quasi-Cyclic Root-LDPC codes for block fading channels," *IEEE Communications Letters*. In press.

[19] A. Lapidoth, "The performance of convolutional codes on the block erasure channel using various finite interleaving techniques," *IEEE Transactions on Information Theory*, vol. 40, no. 5, pp. 1459–1473, 1994.

[20] R. J. McEliece and W. E. Stark, "Channels with block interference," *IEEE Transactions on Information Theory*, vol. 30, no. 1, pp. 44–53, 1984.

[21] T. J. Richardson, M. A. Shokrollahi, and R. L. Urbanke, "Design of capacity-approaching irregular low-density parity-check codes," *IEEE Transactions on Information Theory*, vol. 47, no. 2, pp. 619–637, 2001.

[22] J. J. Boutros, A. G. I. Fàbregas, E. Biglieri, and G. Zémor, "Low-density parity-check codes for nonergodic block-fading channels," *IEEE Transactions on Information*, vol. 56, no. 9, pp. 4286–4300, 2009.

[23] J. Thorpe, "Low-density parity-check (LDPC) codes constructed from protographs," *JPL INP Progress Report*, vol. 42, no. 154, pp. 1–7, 2003.

[24] W. Ryan and S. Lin, *Channel Codes, Classical and Modern*, Cambridge University Press, Cambridge, UK, 2009.

[25] D. Tse and P. Viswanath, *Fundamentals of Wireless Communication*, Cambridge University Press, Cambridge, UK, 2005.

[26] G. I. Fàbregas, "Coding in the block-erasure channel," *IEEE Transactions on Information Theory*, vol. 52, no. 11, pp. 5116–5121, 2006.

[27] E. Biglieri, J. Proakis, and S. Shamai, "Fading channels: information-theoretic and communications aspects," *IEEE Transactions on Information Theory*, vol. 44, no. 6, pp. 2619–2692, 1998.

[28] G. Ungerboeck, "Channel coding with multilevel/phase signals," *IEEE Transactions on Information Theory*, vol. 28, no. 1, pp. 55–67, 1982.

[29] M. Abramowitz and I. Stegun, *Handbook of Mathematical Functions: with Formulas, Graphs, and Mathematical Tables*, Courier Dover, New York, NY, USA, 1965.

[30] D. Duyck, D. Capirone, M. Moeneclaey, and J. J. Boutros, "A full-diversity joint network-channel code construction for cooperative communications," in *Proceedings of the IEEE International Symposium on Personal, Indoor and Mobile Radio Communications (PIMRC '09)*, 2009.

[31] T. Richardson and R. Urbanke, "The capacity of low-density paritycheck codes undermessage-passing decoding," *IEEE Transactions on Information Theory*, vol. 47, no. 2, pp. 599–618, 2001.

[32] H. Jin, T. Richardson, F. Technol, and N. Bedminster, "Block error iterative decoding capacity for LDPC codes," in *Proceedings of the IEEE International Symposium on Information Theory (ISIT '05)*, pp. 52–56, 2005.

[33] M. Lentmaier, D. V. Truhachev, K. S. Zigangirov, and D. J. Costello Jr., "An analysis of the block error probability performance of iterative decoding," *IEEE Transactions on Information Theory*, vol. 51, no. 11, pp. 3834–3855, 2005.